TOWARDS A STRUCTURE-BASED MODEL FOR THE PREDICTION OF PASSIVE SCALAR TRANSPORT IN HYDRODYNAMIC AND MHD TURBULENCE SHEARED IN FIXED AND ROTATING FRAMES

Stavros C. Kassinos
Department of Mechanical and Manufacturing Engineering,
University of Cyprus
Kallipoleos 75, 1678 Nicosia, Cyprus
kassinos@ucy.ac.cy

Evangelos E. Akylas
Department of Mechanical and Manufacturing Engineering,
University of Cyprus
Kallipoleos 75, 1678 Nicosia, Cyprus
akylas@ucy.ac.cy

ABSTRACT

Turbulence models for passive scalar transport are known to have difficulties in complex flows involving strong rotation or MHD effects. Here, we consider the transport of a passive scalar in homogeneous turbulence examined in rotating frames. We first examine the effects of system rotation in the case of decaying hydrodynamic turbulence using Rapid Distortion Theory (RDT) as a guide. It is shown that the evolution of the scalar flux is strongly influenced by the structure dimensionality of the flow, and this suggests that scalar flux models must be made structure aware. Then, using Direct Numerical Simulations (DNS), we proceed to examine the case of passive scalar transport under the influence of homogeneous MHD turbulence in a conducting fluid that is undergoing mean shear in fixed and rotating frames. It is shown that in all the cases considered here, the evolution of the scalar flux coefficients can be explained in terms of the structural information provided by the one-point structure tensors. These results provide strong support for the formulation of structure-based models for passive scalar transport.

INTRODUCTION

The transport and dispersion of scalars in turbulent flows is important in many engineering applications, such as pollutant dispersion and heat transfer in turbomachinery. Many magnetohydrodynamic (MHD) shear flows of engineering or scientific interest also involve the transport and dispersion of passive scalars. For example, liquid metal flows in fusion reactor blankets are complicated by the intricacies of the geometry and the presence of thermal gradients and curvature. There are also important examples, where scalar transport takes place in an MHD fluid that is being sheared in a rotating system. For example, the transport of internal energy is important in the workings of the Earth's dynamo, and plays a key role in stellar accretion disks, in the interstellar medium, and other astrophysical settings as well.

There is clearly a need for turbulence models that can provide robust and reliable predictions of scalar transport in the presence of complex dynamical effects, such as system rotation or magnetic fields. The transport of a passive scalar in homogeneous shear flow offers a simplified setting where new modeling ideas can be developed and tested.

A recent DNS study of homogeneous shear in a rotating frame by Brethouwer (2005) has provided valuable insight into the modifications that system rotation induces on scalar transport. Both the scalar transport rate and the direction of the scalar flux were shown to depend strongly on the ratio of the frame rotation rate to the mean shear rate. In another recent study, Kassinos et al. (2006) examined the evolution of homogeneous MHD turbulence that was being sheared in fixed and rotating frames. They found that the structure of the evolving turbulence fields was strongly dependent on the various ratios of the characteristic time scales of the mean shear, the frame rotation and the magnetic field. Kassinos et al. (2007) used DNS to examine passive scalar transport in a conducting liquid being sheared in a rotating frame while being exposed to a uniform external magnetic field. In the case when the time scale of the mean shear was 20 times larger than the Joule time scale of the magnetic field, they found that the scalar transport was closely linked to the structure of the turbulence field.

Here we first use Rapid Distortion Theory (RDT) to examine passive scalar transport in hydrodynamic homogeneous turbulence that is decaying in a rotating frame. Then, we use DNS to establish the connection between the turbulence structure and scalar transport in a conducting fluid that is exposed to a uniform external magnetic field while being sheared in fixed and rotating frames. In the MHD case, we take the time scale of the mean shear to be comparable to the magnetic Joule time scale, because this leads to a rich interplay of dynamical effects (Kassinos et al., 2006).

THE ONE-POINT TURBULENCE STRUCTURE TENSORS

The Reynolds stress tensor

$$R_{ij} =< u_i u_j > \qquad q^2 = 2\kappa = R_{ii} \qquad r_{ij} = R_{ij}/q^2 \quad (1)$$

where and κ is the turbulent kinetic energy, describes the componentality of the turbulence, giving information on how energetic the velocity fluctuations are in different directions.

It does not, however, provide information on how these fluctuations are organized in structures. The diagnostic tool used for determining the structural morphology of the turbulence fields are the one-point structure-tensors introduced by Kassinos et al. (2001). In homogeneous turbulence, the structure dimensionality tensor is

$$D_{ij} = \int E_{nn}(k)\ \frac{k_i k_j}{k^2} d^3\mathbf{k},\ d_{ij} = D_{ij}/D_{kk},\ D_{kk} = q^2 \quad (2)$$

where $E_{ij}(k) \sim< \hat{u}_i \hat{u}_j^* >$ is the velocity spectrum tensor, k_i are the components of the wavenumber vector. One can show (Kassinos and Reynolds, 1995) that, in the limit of RDT, mean rotation has only a kinematic effect on D_{ij}. Hence, in the case of decaying turbulence in a rapidly rotating frame (no mean deformation), D_{ij} remains unaffected by the frame rotation, as is the case with the turbulent kinetic energy. Note that each diagonal component of d_{ij} can attain values only between 0 and 1, and that in an isotropic field all three diagonal components are equal to each other ($d_{11} = d_{22} = d_{33} = \frac{1}{3}$). For turbulence in which the energy-containing structures are elongated in the x_α direction, $d_{\alpha\alpha} \to 0$, while $d_{\alpha\alpha} \to 1$ corresponds to structures that are narrow and have strong gradients in the x_α direction. We also use the structure circulicity tensor

$$F_{ij} = \int \frac{W_{ij}(k)}{k^2}\, d^3\mathbf{k}, \quad f_{ij} = F_{ij}/F_{kk}, \quad F_{kk} = q^2 \quad (3)$$

where $W_{ij} \sim< \hat{\omega}_i \hat{\omega}_j^* >$ is the vorticity spectrum tensor. F_{ij} describes the large-scale circulation in the field. For example, when all of the large-scale circulation is concentrated, let's say, around the x_1 axis, $f_{11} = F_{11}/F_{ii} \to 1$. In homogeneous turbulence, the Reynolds stress, dimensionality and circulicity tensors are related through the constitutive equation

$$R_{ij} + D_{ij} + F_{ij} = q^2 \delta_{ij} \quad \text{or} \quad r_{ij} + d_{ij} + f_{ij} = \delta_{ij} \quad (4)$$

where in writing the second equation in (4), we have used the fact that in homogeneous turbulence $R_{ii} = D_{ii} = F_{ii} = q^2$.

LINEAR ANALYSIS OF A HYDRODYNAMIC CASE

The inviscid RDT transport equations for the fluctuating velocity components u_i, in the case of turbulence decaying without deformation in a frame rotating about the x_3 axis, become

$$\dot{u}_i = -p_{,i}/\rho_0 + 2\epsilon_{ij3}\Omega^f u_j \quad (5)$$

where Ω^f is the frame rotation rate. Hereafter, we are using index notation, where a subscript following a comma denotes spatial differentiation. The Fourier transformed variables (denoted with $\hat{}$) evolve according to

$$d\hat{u}_i/d\tau = i\hat{p}k_i/\rho_0 + 2\epsilon_{ij3}\Omega^f \hat{u}_j \quad (6)$$

Applying the Fourier transformed continuity equation, $k_i\hat{u}_i = 0$, in (2), we can solve for the pressure

$$ik^2\hat{p}/\rho_0 = -2\Omega^f k_1 \hat{u}_2 + 2\Omega^f k_2 \hat{u}_1 \quad (7)$$

and by substituting into the system (2), this simplifies to

$$d\hat{u}_i/d\beta = \epsilon_{nm3}(k_i k_n/k^2 - \delta_{in})\hat{u}_m \quad (8)$$

where k_i are the components of the wavenumber vector, $k^2 = k_1^2 + k_2^2 + k_3^2$, and $\beta = 2\Omega^f$ is the total rotation applied. The solution of the above system takes totally different forms depending on the dimensionality of the turbulence. For example, for the initially isotropic 3D-3C case it has been shown that the Reynolds stresses remain constant (but not the instantaneous velocities). However this behavior may change significantly for different initializations, depending on the dimensionality tensor (Reynolds, 1989; Kassinos et al., 2001). Below we show an example for two-dimensional (2D) turbulence where the axis of independence is aligned either with the axis of rotation x_3, and thus $d_{33} = 0$, or with the axis x_1 normal to the rotation axis, and thus $d_{11} = 0$. Using linear analysis, we show that the scalar fluctuations θ of a passive scalar Θ, with a constant mean gradient $\Gamma_i = \Theta_{,i}$, follow a significantly different evolution history depending on the dimensionality of the turbulence.

The evolution of the Fourier transformed scalar fluctuations for our case is governed by

$$d\hat{\theta}/d\beta = -\gamma_m \hat{u}_m \quad (9)$$

where $\gamma_m = \Gamma_m/(2\Omega^f)$. In order to calculate and integrate the 2D spectra for the derivation of the Reynolds stresses and the scalar fluxes, we make use of two different initializations, namely a vortical and a jetal initial velocity spectrum (Kassinos et al., 2001; Akylas et al., 2007). More specifically, in the vortical case the componentality of the initially 2D turbulence is isotropic in planes perpendicular to the axis of independence x_α. In this case, the vortical 2D-2C (see also Cambon et al., 1997) spectrum is given by

$$E_{ij}^{vor} = \frac{E(k,0)}{2\pi k}\delta(k_\alpha)(\delta_{ij} - \frac{k_i k_j}{k^2}) \quad (10)$$

with i and j allowed to take all the values 1,2,3, apart from the value of α. In contrast, when the initial turbulence is completely jetal, all the velocity fluctuations are in the direction of the axis of independence x_α. The initial 2D-1C jetal spectrum corresponding to this condition is

$$E_{ij}^{jet} = \frac{E(k,0)}{2\pi k}\delta_{i\alpha}\delta_{j\alpha} \quad (11)$$

with i and j taking only the value of α (no summation implied for repeated Greek indices). In the relations (6) and (7) the initial turbulent kinetic energy spectrum satisfies

$$\int_{k=0}^{\infty} E(k,0)dk = \frac{q_0^2}{2} = \frac{R_{nn}}{2} \quad (12)$$

Because of the linearity of the governing equations, the solutions for the initially jetal 2D-1C and the initially vortical 2D-2C cases can be superposed to produce the turbulence statistics for various 2D-3C initial fields, consisting of uncorrelated jets and vortices.

2D Case with $k_1 = 0$

In this case the turbulence is independent of the x_1-axis and consists of very long axisymmetric structures ($d_{22} = d_{33} = 0.5$) aligned with the x_1 direction. The solution of (4) for the Fourier transformed velocity components becomes

$$\begin{aligned} \hat{u}_1 &= \hat{u}_1^0 \cos(\beta \sin\phi) + \hat{u}_2^0 \csc\phi \sin(\beta \sin\phi) \\ \hat{u}_2 &= \hat{u}_2^0 \cos(\beta \sin\phi) - \hat{u}_1^0 \sin\phi \sin(\beta \sin\phi) \\ \hat{u}_3 &= \hat{u}_3^0 \cos(\beta \sin\phi) + \hat{u}_1^0 \cos\phi \sin(\beta \sin\phi) \end{aligned} \quad (13)$$

In the above we have set $k_2 = k\cos\phi, k_3 = k\sin\phi$ in cylindrical coordinates. In the case of a passive scalar with a constant mean gradient in x_2 direction $\Theta = \Gamma_2 x_2$, the integration of (5) for zero initial scalar fluctuations gives

$$\hat{\theta} = -\gamma_2 \hat{u}_1^0(\cos(\beta \sin\phi) - 1) - \gamma_2 \hat{u}_2^0 \csc\phi \sin(\beta \sin\phi) \quad (14)$$

Forming the 2D-3C spectra, superposing 2/3 of (6) and 1/3 of (7), and integrating over k_2 and k_3, we calculate the Reynolds stresses

$$\begin{aligned}\frac{R_{11}}{q_0^2} &= \frac{3-2J_0(2\beta)}{6}\\ \frac{R_{22}}{q_0^2} &= \frac{3+2J_0(2\beta)-J_1(2\beta)/\beta}{12}\\ \frac{R_{33}}{q_0^2} &= \frac{3+J_1(2\beta)/\beta}{12}\end{aligned} \tag{15}$$

where J_n are Bessel functions of the first kind. Unlike the 3D initially isotropic case, where the turbulent stresses remain isotropic, for this 2D case the stresses evolve, showing an oscillatory behavior around the values $r_{11} = 1/2$, $r_{22} = r_{33} = 1/4$, as it is illustrated in Fig. 1.

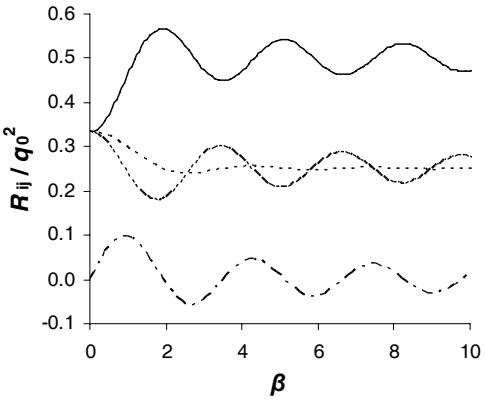

Figure 1: Evolution of the Reynolds stresses for the 2D case with independence of x_1-axis ($d_{11} = 0$): 11 (solid), 22 (short dashed), 33(long dashed) and 12 (dot-dashed).

Similarly, the integrations for the passive scalar fluxes yield

$$\begin{aligned}\frac{\overline{u_1\theta}}{\gamma_2 q_0^2} &= \frac{-3+J_0(2\beta)+2J_0(\beta)}{6}\\ \frac{\overline{u_2\theta}}{\gamma_2 q_0^2} &= \frac{J_1(2\beta)-2J_1(\beta)}{6}\\ \frac{\overline{u_3\theta}}{\gamma_2 q_0^2} = 0 \quad \frac{\overline{\theta^2}}{\gamma_2^2 q_0^2} &= \frac{5-J_0(2\beta)-4J_0(\beta)}{6}\end{aligned} \tag{16}$$

Following the notation of Brethouwer (2005) and Rogers et al. (1989), the scalar-velocity correlation coefficient is defined by

$$\zeta_\beta^\alpha = \overline{u_\beta \theta_\alpha}/u'_\beta \theta'_\alpha \tag{17}$$

where $u'_\beta = \sqrt{R_{\beta\beta}}$ and $\theta'_\alpha = \sqrt{\overline{\theta^2}}$ are the rms velocity and scalar fluctuations, the index α denotes the direction of the mean scalar gradient, the index β the direction of the velocity component, and where no summation is implied for repeated Greek indices. Thus, ζ_1^2 characterizes the turbulent flux in the flow direction (x_1) of a scalar with an imposed mean scalar gradient in the transverse (cross flow) direction (x_2), and consequently, the correlation coefficients for the scalar fluxes become

$$\begin{aligned}\zeta_2^2 &= \frac{\sqrt{2}(J_1(2\beta)-2J_1(\beta))}{\sqrt{(5-J_0(2\beta)-4J_0(\beta))(3+2J_0(2\beta)-J_1(2\beta)/\beta)}}\\ \zeta_1^2 &= \frac{-3+J_0(2\beta)+2J_0(\beta)}{\sqrt{(5-J_0(2\beta)-4J_0(\beta))(3-2J_0(2\beta))}}\\ \zeta_3^3 &= 0\end{aligned} \tag{18}$$

2D Case with $k_3 = 0$

In this case, the 2D turbulence is independent of the axis of the frame rotation and the Reynolds stresses do not depend on the frame rotation, in agreement with the principle of material indifference (Speziale, 1981). The system (4) yields constant velocity components

$$\hat{u}_i = \hat{u}_i^0 \tag{19}$$

Thus, the Reynolds stresses do not evolve (as in the 3D isotropic case) and the stresses remain fixed to the value $r_{11} = r_{22} = r_{33} = 1/3$. However, through equation (5), the passive scalar fluctuations evolve linearly with time

$$\hat{\theta} = -\gamma_2 \beta \hat{u}_2^0 \tag{20}$$

The integrations over k_1 and k_2 for the calculation of the scalar fluxes show that for this 2D-3C case

$$\frac{\overline{u_1\theta}}{\gamma_2 q_0^2} = 0, \quad \frac{\overline{u_2\theta}}{\gamma_2 q_0^2} = -\frac{\beta}{3}, \quad \frac{\overline{u_3\theta}}{\gamma_2 q_0^2} = 0, \quad \frac{\overline{\theta^2}}{\gamma_2^2 q_0^2} = \frac{\beta^2}{3} \tag{21}$$

The correlation coefficients for the scalar fluxes in this case are zero apart from the scalar flax in the x_2 direction

$$\zeta_1^2 = 0 \qquad \zeta_2^2 = -1 \qquad \zeta_3^2 = 0 \tag{22}$$

In Fig. 2 we show a comparison between the correlation coefficients for the scalar fluxes corresponding to the 3D-3C isotropic case, and the 2D-3C cases with $d_{11} = 0$ and with $d_{22} = 0$. The results for the 3D-3C isotropic case have been calculated using the PRM (Kassinos and Reynolds, 1999).

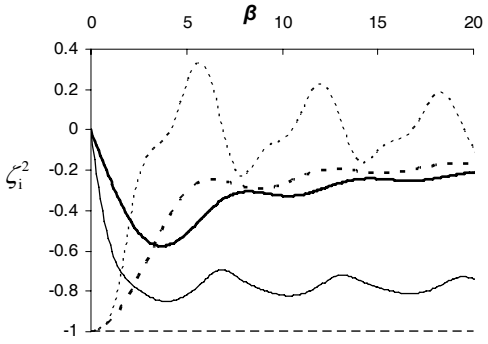

Figure 2: Evolution of correlation coefficients for the scalar fluxes $\overline{u_i\theta}$ for the initially 3D-3C isotropic case (bold lines: i=1, solid, and i=2, dashed), the 2D case with independence of x_1-axis ($d_{11} = 0$) (thin lines: i=1, solid, and i=2, dashed) and the 2D case with independence of x_3-axis ($d_{33} = 0$) (thin line: i=2, long-dashed).

From the comparisons it is clear that for the isotropic case the correlations gradually vanish. For the two 2D cases a strong correlation survives at large β. In the case with

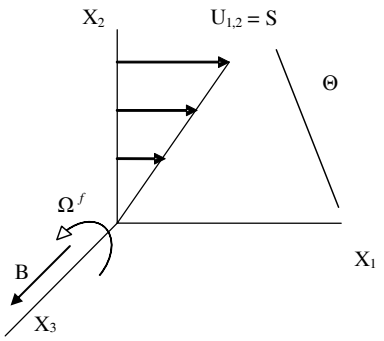

Figure 3: Flow configuration

$d_{11} = 0$ the surviving correlation is $\overline{u_1\theta}$, while in the case with $d_{33} = 0$ is $\overline{u_2\theta}$.

This simple linear analysis has shown that the structure dimensionality of the turbulence has a strong effect on passive scalar transport. Next, we use DNS to examine the relation between the dimensionality of the turbulence structure and passive scalar transport in complex flows.

DIRECT NUMERICAL SIMULATIONS OF MHD CASES

Here we discuss only the case where both the frame rotation and the imposed magnetic field are aligned with the spanwise direction (normal to the plane of the mean shear) as shown in Fig. 3. A uniform mean passive scalar gradient is imposed in the transverse direction (normal to the streamwise within the plane of the mean shear). The hydrodynamic configuration is relevant to several engineering applications, including turbomachinery and geophysical flows, while the MHD configuration is relevant to accretion disks. We take the mean deformation tensor, the frame rotation, imposed magnetic field, and mean scalar gradient vectors to be

$$G_{ij} \equiv U_{i,j} = S\delta_{i1}\delta_{j2} \qquad \Omega_i^f = \Omega^f \delta_{i3}$$
$$B_i = B\delta_{i3} \qquad \Gamma_i \equiv \Theta_{,i} = \Gamma\delta_{i2} \tag{23}$$

where U_i and Θ are the mean velocity and the mean scalar.

Dimensionless parameters

The effects of a uniform magnetic field applied to unstrained homogeneous turbulence in an electrically conductive fluid are characterized by three dimensionless parameters. The first of these is the magnetic Reynolds number

$$R_m = \frac{v'L}{\eta} = (\frac{v'}{L})(\frac{L^2}{\eta}) \tag{24}$$

where L is the integral length scale, $v' = \sqrt{R_{ii}/3}$ is the rms velocity and η is the magnetic diffusivity

$$\eta = 1/(\sigma\mu^*) \tag{25}$$

Here σ is the electric conductivity of the fluid, and μ^* is the fluid magnetic permeability (here we use μ^* for the magnetic permeability and reserve μ for the dynamic viscosity). Thus the magnetic Reynolds number represents the ratio of the characteristic time scale for diffusion of the magnetic field (L^2/η) to the time scale of the turbulence (L/v).

The second parameter is the magnetic Prandtl number representing the ratio of R_m to the hydrodynamic Reynolds number Re_L

$$P_m \equiv \frac{\nu}{\eta} = \frac{R_m}{Re_L}, \qquad Re_L = \frac{v'L}{\nu} \tag{26}$$

Similarly, we can define the scalar Prandtl number $P_s \equiv \nu/\varkappa$, where $\varkappa$ is the scalar diffusivity. Here we assume $P_s = 1$.

The magnetic-interaction number is

$$N \equiv \frac{\sigma B^2 L}{\rho v'} = \frac{(B^{\rm ext})^2}{\eta}\frac{L}{v'} = \frac{\tau}{\tau_m} \tag{27}$$

where B is the magnitude of the magnetic field, $B^{\rm ext} = B/\sqrt{\mu^*\rho}$ is the magnetic field expressed in Alfven units, and ρ is the fluid density. N represents the ratio of the turbulence time scale $\tau = L/v'$ to the Joule time $\tau_m = \eta/(B^{\rm ext})^2$, i.e. the characteristic time scale for dissipation of turbulent kinetic energy by the action of the Lorentz force. N parametrizes the ability of an imposed magnetic field to drive the turbulence to a two-dimensional three-component state.

In the presence of mean shear and frame rotation, two additional parameters become important. The first of these is the ratio of the time scale of the mean shear $\tau_{\rm shear} \equiv 1/S$ to the Joule time τ_m,

$$M \equiv \frac{(B^{\rm ext})^2}{\eta S} = \frac{\tau_{\rm shear}}{\tau_m} \tag{28}$$

where S is the mean shear rate. The second is the ratio of the frame rotation rate Ω^f to shear rate S,

$$\lambda \equiv \frac{2\Omega^f}{S} \tag{29}$$

where $\Omega^f = -\Omega_{12}^f$ so that positive values of λ correspond to a frame counter-rotating relative to the sense of rotation associated with the mean shear (see Fig. 1). With this definition, $\lambda = 1$ corresponds to a frame that counter-rotates at a rate that exactly matches the intrinsic rotation rate associated with mean shear, and $\lambda = 0.5$ to the most unstable case where the turbulent kinetic energy growth rate is maximized.

Finally, the dimensionless shear parameter, which represents the ratio of the turbulence time scale $\tau_{\rm turb} \equiv q^2/\epsilon$ to the mean shear time scale $\tau_{\rm shear} \equiv 1/S$,

$$S^* \equiv \frac{Sq^2}{\epsilon} = 2\frac{Sk}{\epsilon} = \frac{3S(v')^2}{\epsilon} = \frac{\tau_{\rm turb}}{\tau_{\rm shear}} \tag{30}$$

provides a measure of the rapidity of the mean deformation.

Governing equations

Passive scalar transport in homogeneous MHD shear flow is described by the incompressible MHD equations with the addition of the passive scalar transport equation. Here, the governing equations are transformed into a rotating frame, where they are explicitly decomposed into a mean and a fluctuating part. Within the rotating frame, we solve the resulting governing equations for the fluctuation velocity field v_i, the fluctuation magnetic field b_i and the passive scalar fluctuation θ in a coordinate system that deforms with the mean flow, so that Fourier decomposition methods can be employed. In this deforming coordinate system, the transformed equations become

$$\partial_t v_i + G_{ik}v_k + \frac{\partial v_i}{\partial x_m}v_k A_{mk} + 2\Omega_{ik}^f v_k = -\frac{1}{\rho}\frac{\partial p}{\partial x_m}A_{mi} + \frac{\partial B_i^{\rm ext}}{\partial x_m}b_k A_{mk} + \frac{\partial b_i}{\partial x_m}B_k^{\rm ext}A_{mk} + \frac{\partial b_i}{\partial x_m}b_k A_{mk} + \nu\frac{\partial^2 v_i}{\partial x_k \partial x_z}A_{zp}A_{kp} \tag{31}$$

$$\partial_t b_i - G_{ik} b_k = -v_k \frac{\partial B_i^{\rm ext}}{\partial x_m} A_{mk} - v_k \frac{\partial b_i}{\partial x_m} A_{mk}$$

$$+B_k^{\rm ext} \frac{\partial v_i}{\partial x_m} A_{mk} + b_k \frac{\partial v_i}{\partial x_m} A_{mk} + \eta \frac{\partial^2 b_i}{\partial x_k \partial x_z} A_{zp} A_{kp} \quad (32)$$

and

$$\partial_t \theta + \frac{\partial \theta}{\partial x_m} A_{mk} v_k + \Gamma_m A_{mk} v_k = \varkappa \frac{\partial^2 \theta}{\partial x_k \partial x_z} A_{zp} A_{kp} \quad (33)$$

Here, p is the total pressure including a magnetic contribution, B_i are the components of the imposed mean magnetic field, x_i are deforming coordinates, $G_{ij} = U_{i,j}$ is the mean velocity gradient tensor, and A_{ij} is the (Rogallo) transformation matrix (see for example Kassinos and Reynolds, 1995). $\Gamma_i \equiv \Theta_{,i} = \Gamma \delta_{i2}$ is the mean scalar gradient vector, which is taken to be uniform in space and constant in time.

Numerical code and initial conditions

We have used a pseudo-spectral code with the ability to simulate the full MHD equations (31) through (33). The numerical method used to solve the governing equations for homogeneous shear flows is similar to that introduced by Rogallo (1981). In the deforming coordinates, Fourier pseudo-spectral methods, with periodic boundary conditions, are used for the representation of the spatial variation of the flow variables. Time advance is accomplished by a third-order Runge-Kutta method. Since the mean imposed shear skews the computational grid with time, periodic remeshing of the grid is needed in order to allow the simulation to progress to large total shear, where a self-preserving regime might be expected to prevail. The periodic remeshing introduces aliasing errors that are removed by a de-aliasing procedure (Rogallo, 1981) included in the code.

All the runs presented here have a resolution of 256^3 Fourier modes in a $(2\pi)^3$ computational domain. The initial conditions were created starting with a pulse of energy at low wave numbers in Fourier space and a random distribution of phases for the Fourier modes. In order to let the higher-order statistics develop, the flow was evolved in the absence of either mean shear or frame rotation, and without a mean magnetic field or mean scalar gradient, while forcing was being applied to the low wave number region of the spectrum. This initial phase was continued until an equilibrium state was reached and the skewness acquired its peak value. At that time, hereafter referred to as t_0, the external magnetic field, mean scalar gradient, mean shear and frame rotation were switched on, while the artificial forcing was eliminated. The characteristics of the initial field at time t_0 are summarized in Table 1. In all runs, the scalar fluctuation field was initialized to zero at $t = t_0$ and allowed to evolve as result of the interaction with the velocity fluctuations. Thus our initial conditions for the scalar field are the same as those adopted by Brethouwer (2005). Similarly, in the MHD runs, an initial condition for b_i has to be chosen at $t = t_0$. Here we have made the choice $b_i(t_0) = 0$. In other words, our simulations describe the response of an initially non-magnetized turbulent conductive fluid to the application of a mean magnetic field.

For a given initial hydrodynamic field, not all of these parameters can be independently specified. For example, specification of M and N_0 determines the ratio of the turbulence time scale to the mean shear time scale $S_0^* = (3S(v')^2/\epsilon)_0$ as well. Here, we have chosen to set $R_m = 1$, $M = 2$ and $N_0 = 15$ (or $N_0 = 0$ in the hydrodynamic case). The resulting value of $S_0^* = 35.85$ matches closely the conditions considered by Brethouwer (2005), and thus results from the hydrodynamic runs in this group of simulations can be compared directly with the results of Brethouwer, offering a valuable validation of the current simulations. $M = 2$ means that the time scale of the mean shear is comparable to the Joule time, and based on the results of Kassinos et al. (2006), one would expect a rich interplay between the effect of the mean shear and the magnetic field. Finally, it should be noted that for the MHD runs, specification of R_m and N completely determines η and $B^{\rm ext}$ through equations (24) and (27). In all cases, the mean scalar gradient Γ_i is taken to be uniform and aligned with the transverse direction x_2. Through a proper non-dimensionalization of the scalar transport equation (33), it can be shown that the magnitude of Γ_i is irrelevant, and is thus taken to be unity.

Table 1: Turbulence characteristics of the initial velocity field. All quantities are in MKS units.

Resolution	256^3
Box size ($\ell_x \times \ell_y \times \ell_z$)	$2\pi \times 2\pi \times 2\pi$
Rms velocity (v')	1.447
Viscosity	0.006
Integral length-scale (L)	
$(3\pi/4 \times (\int k^{-1} E(k) dk / \int E(k) dk))$	0.357
$Re = vL/\nu$	86
Dissipation (ϵ)	5.334
Dissipation length scale ($\gamma = (\nu^3/\epsilon)^{(1/4)}$)	0.0142
$k_{\max}\gamma$	1.82
Microscale Reynolds number	
$(Re_\lambda = \sqrt{15/(\nu\epsilon)} v^2)$	45.35
Eddy turnover time ($\tau = (3/2)v^2/\epsilon$)	0.589

Results

For the MHD cases considered here it is convenient to define equivalent structure dimensionality tensors for the magnetic and passive scalar fluctuations fields. When the trace of the velocity spectrum tensor $E_{nn}(k)$ in (2) is replaced by the trace of the magnetic spectrum tensor $E^b_{nn}(k) \sim < \hat{b}_n \hat{b}^*_n >$, one obtains an equivalent tensor D^m_{ij} describing the structure of the fluctuating magnetic field. We will use D^m_{ij} as a diagnostic of structure alignment in the magnetic field. In a similar fashion, we define

$$D^s_{ij} = \int E^s(k) \, \frac{k_i k_j}{k^2} \, d^3\mathbf{k}, \; d_{ij} = D^s_{ij}/D^s_{kk}, \; D^s_{kk} =< \theta\theta > \quad (34)$$

and use this as a diagnostic of the structure of the passive scalar field. Here $E^s(k) =< \hat{\theta}\hat{\theta}^* >$.

In most cases, the one-point structure tensors provide all the structural information that is necessary to infer scalar transport. For example, as shown in Figs. 4a,d and 5, in the hydrodynamic case, the velocity and scalar fluctuation fields are organized into long streamwise eddies with an almost axisymmetric cross section ($d_{11} \approx 0.1, d_{22} \approx 0.4, d_{33} \approx 0.5$). In the $R_m = 1$ MHD case, the streamwise structures in the velocity field become flattened, with a cross section that is much narrower in the spanwise than in the transverse direction ($d_{11} \approx 0, d_{22} \approx 0.3, d_{33} \approx 0.7$). A similar morphology is found in the magnetic fluctuation field. To understand the behavior of the scalar flux coefficient (equation 17) shown in Fig. 6c, we examine in greater detail the turbulence structure tensor for the velocity field. As shown in Figs. 5 and 6, in the absence of a magnetic field, the streamwise eddies have a very strong vortical character ($r_{11} << r_{22}, r_{33}$, $f_{11} \approx 8.3$ at $St = 10$). As one would have

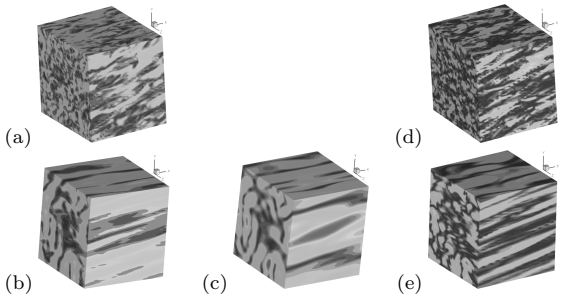

Figure 4: Three dimensional magnitude contours showing the structural anisotropy induced at large times ($St = 10$) when $R_m = 1$, $M = 2$ and $\lambda = 1$: (a) Velocity field for the hydrodynamic case; (b) velocity field for MHD case; (c) magnetic field case the MHD case; (d) scalar field case hydrodynamic case; (e) scalar field case the MHD case;

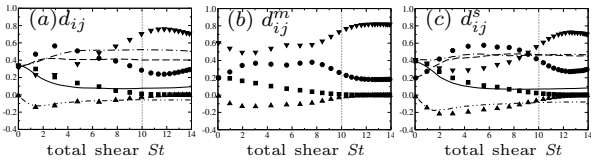

Figure 5: Evolution of the normalized dimensionality tensor for (a) the velocity field, (b) the magnetic field, and (c) the scalar field when $\lambda = 1.0$. Lines correspond to the hydrodynamic case and dark symbols to the MHD ($R_m = 1$) case: (■ , ———) d_{11}; (● , – – – –) d_{22}; (▼ , —·—) d_{33}; (▲ , —··—) d_{12}.

expected, this strongly vortical organization of the velocity field, favors a strong scalar flux in the transverse direction and ζ_2^2 is quite large at $St = 10$, while the streamwise flux coefficient is almost zero (see Fig.6c). In the $R_m = 1$ MHD case, the flattened streamwise eddies are no longer vortical, but instead represent helical structures where kinetic energy is equally distributed among jetal and vortical motions ($r_{11} \approx r_{22} \approx 0.4$ at $St = 10$ in Fig. 6). In addition, the flattening ($d_{22} << d_{33}$) of the eddy cross section (which appears much wider the in transverse direction x_2) favors the coherence of the turbulent fluctuation in that direction. As a result, the scalar flux coefficients in both the streamwise and transverse directions are quite large at $St = 10$.

The above discussion shows that the drastic modifications of the scalar flux coefficients induced by the external magnetic field can be explained nicely if one makes use of the one-point turbulence structure tensors (2), (3) and (34) in order to visualize the morphology of the turbulence fields.

CONCLUSIONS

We have used Rapid Distortion Theory (RDT) and Direct Numerical Simulations (DNS) to show that the transport of a passive scalar in both simple hydrodynamic, and in more complex flows, is to a large extend determined by the structure of the turbulent fields. Furthermore, the one-point turbulence structure tensors were shown to provide an accurate description of the structural morphology of the turbulence. In the case of MHD turbulence in a rotating frame, the structure tensors were used to explain modifications in passive scalar flux, brought about by the activation of the external magnetic field, that would otherwise be difficult to understand. We propose that these results provide strong evidence for the need to construct structure-based models

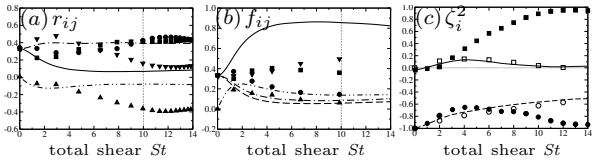

Figure 6: Evolution of (a) r_{ij} (equation 1) and (b) of f_{ij} (equation 3) when $\lambda = 1.0$. Lines correspond to the hydrodynamic case and dark symbols to the MHD case with $R_m = 1$: (■ , ———), 11 component; (● , – – – –), 22 component; (▼ , —·—), 33 component; (▲ , —··—), 12 component. The corresponding evolution of the scalar flux coefficient (equation 17) is shown in (c); lines correspond to the hydrodynamic case, dark symbols to the MHD case, and open symbols to the hydrodynamic simulations of Brethouwer (2005): (□ , ■ , – – – –) ζ_1^2; (○ , ● , ———) ζ_2^2.

for the turbulent flux of passive scalars. We are currently working on the construction of such a structure-based model and we hope to soon be able to report on its performance.

REFERENCES

Akylas, E., Kassinos, S.C., and Langer, C.A., 2006, "Analytical solution for a special case of rapidly distorted turbulent flow in a rotating frame", *Phys. Fluids*, Vol. 18, 085104.

Akylas, E., Kassinos, S.C., and Langer, C.A., 2007, "Rapid shear of initially anisotropic turbulence in a rotating frame", *Phys. Fluids*, Vol. 19, 025102.

Brethouwer, G., 2005, "The effect of rotation on rapidly sheared homogeneous turbulence and passive scalar transport. Linear theory and direct numerical simulation", *J. Fluid Mech.*, Vol. 542, pp. 305-342.

Cambon, C., Mansour, N.N., and Godeferd, F.S., 1997, "Energy transfer in rotating turbulenc", *J. Fluid Mech.*, Vol. 337, pp. 303-332.

Kassinos, S. C. and Reynolds, W. C., 1995, "A structure-based model of the rapid distortion of homogeneous turbulence", Tech. Rep. TF-61, Mechanical Engineering Department, Stanford University.

Kassinos, S. C., and Reynolds, W. C., 1999, "Structure-based modeling for homogeneous MHD turbulence". *Annual Research Briefs 1999*, pp. 301-315. Stanford Univ./NASA Ames Res. Center: Center for Turbulence Research.

Kassinos, S. C., Reynolds, W.C., and M. M. Rogers, M. M., 2001, "One-point turbulence structure tensors", *J. Fluid Mech.*, Vol. 428, pp. 213-248.

Kassinos, S. C., Knaepen, B., and Wray, A., 2006, "MHD turbulence at moderate magnetic Reynolds number", *J. of Turbulence*, Vol. 7(26).

Kassinos, S. C., Knaepen, B., and Carati, D., 2007, "The transport of a passive scalar in MHD turbulence subjected to mean shear and frame rotation", *Phys. Fluids*, Vol. 19(1), 015105.

Reynolds, W.C., 1989, "Effects of rotation on homogeneous turbulenc", *Proc. 10th Australasian Fluid Mechanics Conference*, University of Melbourne: Melbourne, Australia.

Rogallo, R.S., 1981, "Numerical experiments in homogeneous turbulence". NASA Tech. Memo. 81315.

Speziale, C.G., 1981, "Some interesting properties of two-dimensional turbulence", Phys. Fluids, Vol. 24(8), pp. 1425-1427.